Asian Journal of Chemistry; Vol. 31, No. 4 (2019), 855-859

ASIAN JOURNAL OF CHEMISTRY

https://doi.org/10.14233/ajchem.2019.21814

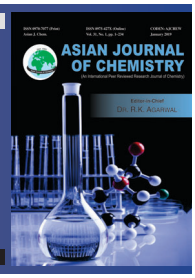

Effect of TiO_2 Concentration on Thermal Stability and Dielectric Properties of $(PANI)_{1-x}(TiO_2)_x$ Nanocomposites

AJAY KUMAR SHARMA[1,2,*], PRAVEEN KUMAR JAIN[3], RISHI VYAS[2] and VIPIN KUMAR JAIN[1]

[1]Institute of Engineering and Technology, JK Lakshmipat University, Jaipur-302026, India
[2]Department of Physics, Swami Keshvanand Institute of Technology, Management & Gramothan, Jaipur-302017, India
[3]Department of Electronics & Communication Engineering, Swami Keshvanand Institute of Technology, Management & Gramothan, Jaipur-302017, India

*Corresponding author: E-mail: ajaymnit19@gmail.com

Received: 13 November 2018; *Accepted*: 26 December 2018; *Published online*: 27 February 2019; AJC-19298

The current paper deals with investigation of $(PANI)_{1-x}(TiO_2)_x$ nanocomposites to explore possible material for optoelectronic devices. To investigate the effect of TiO_2 concentration on structural, surface morphology and chemical properties of PANI, samples were characterized by XRD, FTIR, SEM and Raman spectroscopy. The XRD pattern evidence the presence of a blend of anatase and rutile phase of TiO_2 within the PANI matrix which shows amorphous nature of the matrix. FTIR and Raman spectra confirm the formation of PANI/TiO_2 nanocomposites. SEM images show the appearance of lumps into smooth PANI samples with addition of TiO_2 nanoparticles. The thermal and dielectric properties were studied using TGA and Impedance analyzer, respectively. The results showed that the addition of TiO_2 improves the thermal stability, which clearly shows its potential application in optoelectronic devices.

Keywords: PANI/TiO_2 nanocomposite, Thermal Stability, Dielectric properties.

INTRODUCTION

In recent past, the conducting polymers have been employed widely in diverse fields such as chemical and biological sensors, optoelectronic devices (such as solar cell, LEDs, lasers), actuators microelectronic devices and lightweight batteries [1-5]. Polyaniline (PANI) is one of a versatile conducting polymers owing to its unique properties such as high environmental stability, low cost and good electrical conductivity [6-11]. The electrical properties of PANI can be altered by using protonation and/or charge transfer doping [12,13]. Such materials carry utmost importance in integrated electronic circuits such as capacitor and gate oxides. However, the bottleneck of usage of PANI lies in its thermal instability, weak dielectric properties and poor biocompatibility. To eradicate such incompatibility, the nanocomposites incorporating metal oxides could present a better solution due to the higher thermal stability and average conductivity. TiO_2 is one such wide band-gap (3.2 eV) metal oxide with acceptable utility in both opto-electronic and micro-electronic devices applications exhibiting better mechanical flexibility, thermal and environmental stability [14-18].

Consequently, it is hoped to obtain new materials with complementary behavior between PANI and TiO_2. The composite structure of PANI and TiO_2 have received much consideration due to dissociation of exciton at the interface of TiO_2 and conjugated polymer [19]. Although there are many studies on PANI/TiO_2 composite structure but most of these reports are still focused on material preparation and morphology characterization, such as size and shape of the oxide particles, degree of dispersion, type of interaction, and interface between the organic and inorganic phase [20,21]. Thermal stability of PANI can be enhanced by introducing TiO_2. However, addition of TiO_2 decreases the conductivity of nanocomposite [22]. Therefore, the selection of appropriate concentration of TiO_2 must be selected carefully by balancing thermal stability and electrical conductivity. Keeping in mind the expected potential applications of PANI/TiO_2 nanocomposite, thermal and dielectric properties have been discussed in this article with the variation in the concentration of TiO_2 in resulting nanocomposite with PANI.

EXPERIMENTAL

Pure polyaniline (PANI) was synthesized by *in situ* chemical oxidative polymerization method at lower temperature between 0-5 ºC, which has been reported earlier [23,24]. The $(PANI)_{1-x}(TiO_2)_x$ nanocomposite (x = 0, 0.02, 0.04, 0.08) were prepared *in situ* by chemical oxidation polymerization of aniline using APS as an oxidant in presence of appropriate amount of colloidal TiO_2 nanoparticles at 0-5 ºC in air. The phase and orientation of PANI/TiO_2 nanocomposites were characterized by X-ray diffractometry (XRD, Bruker AXS D-8 Advance Diffractometer) using CuKα (λ = 1.5407 Å) radiation. The surface morphology of the prepared samples is investigated by means of scanning electron microscopy (SEM) using quanta Fe-SEM 450 (FEI). Raman spectra of PANI/TiO_2 nanocomposites were measured using confocal Raman microscopy. FTIR spectroscopy analysis of PANI/TiO_2 nanocomposites scanned from 4000 cm^{-1} to 500 cm^{-1} using a perkin Elmer FTIR spectroscopy. Dielectric properties of nanocomposites were studied using impedance analyzer (Agilent 4294A precision). To measure the thermal stability, Thermogravimetric analysis (Perkin Elmer STA 6000) was done for PANI and PANI/TiO_2 nanocomposites.

RESULTS AND DISCUSSION

The pure PANI and PANI/TiO_2 (8 % w/w) nanocomposite were characterized by X-ray diffraction and the resulting diffraction pattern is plotted (Fig. 1). The diffraction pattern corresponding to pure PANI does not yield into any high intensity peaks and regarded as X-ray amorphous, however, multiple diffraction peaks are observed in spectra of nanocomposite. The diffraction pattern of nanocomposite PANI/TiO_2 (8 % w/w) is indicative of diffraction peaks originating from lattice planes (101-A), (004-A) and (200-A) at diffraction angles (2θ) of 25.38º, 37.88º and 48.07º of anatase phase of TiO_2. Further, other high intensity diffraction peak at diffraction angle of 27.40º indicates the diffraction of X-rays from (110-R) lattice plane of rutile phase of TiO_2. The rest of spectra are identical to pure PANI which indicate no crystallization/change of phase during the preparation of PANI/TiO_2 nanocomposite.

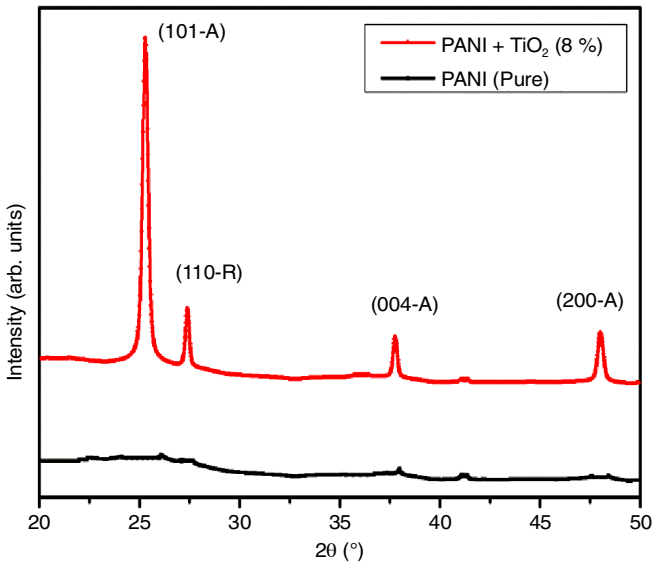

Fig. 1. X-ray diffraction patterns of Pure PANI and PANI/TiO_2 (8%) nanocomposite

The crystallites size of PANI/TiO_2 nanocomposites was estimated from the prominent peak indexed (101-A) having a FWHM of 0.215º using Debye-Scherrer equation [3]:

$$t = \frac{0.9\lambda}{\beta\cos\theta} \quad (1)$$

where β = FWHM (full width at half maxima of diffraction peak in radians.), t = grain size, λ = wavelength of X-ray (Cuk_α used in the present study) and cos θ is the cosine of Bragg angle (θ). The estimated grain size of PANI/TiO_2 nanocomposite was 40.88 nm.

The surface morphology of pure PANI and PANI/TiO_2 (8 % w/w) nanocomposite is recorded using scanning electron microscopy (SEM). Fig. 2a displays the SEM image of pure PANI which is indicative of relatively flat and uniform structure with some coalesce grains. Fig. 2b is a indicative of formation of many uneven lumps in PANI/ TiO_2 (8 % w/w) nanocomposite which is result of incorporation of TiO_2. The polymerization

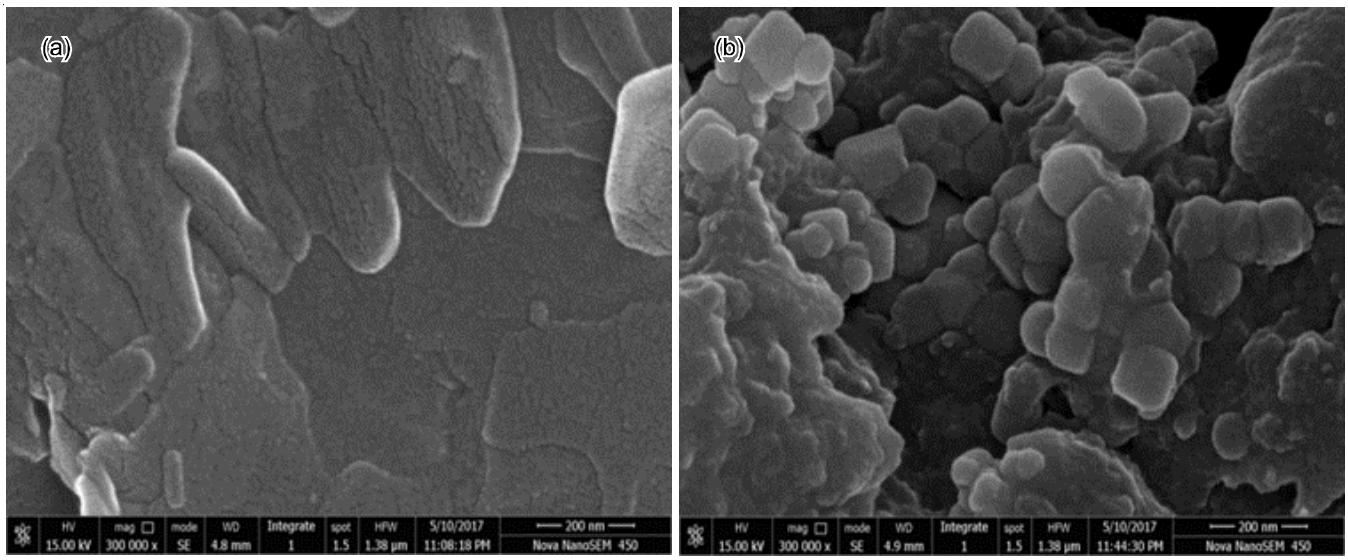

Fig. 2. SEM image of (a) pure PANI and (b) PANI/TiO_2 (8 % w/w) nanocomposite

of aniline has taken place on the surface of TiO_2 nanoparticles which has resulted into visible lumps with TiO_2 at its core. Further, the presence of similar lumps throughout the surface indicate uniform distribution of TiO_2 in nanocomposite.

To indentify the change in the molecular structure of PANI and PANI/TiO_2 nanocomposite, Fourier transform-infrared (FTIR) spectroscopy was used and obtain results are shown in Fig. 3. The characteristics peaks of PANI are evident in all the patterns corresponding to pure PANI and PANI/TiO_2 nanocomposites. The characteristic features of pure PANI is located at 3423, 1628 and 1133 cm^{-1}. The signature of N-H stretching is observed as a peak at 3423 cm^{-1} while the band at 1628 cm^{-1} is recognized as C=N stretching mode of vibration for the quinonoid and benzenoid units of polyaniline [25,26]. The band at 1133 cm^{-1} is allocated to the C-N stretching mode of benzenoid ring which is the indicative of conducting protonated form of polyaniline. The bands in the region 1133-1000 cm^{-1} are due to in-plane bending vibration of C-H mode [27]. The low wave number region exhibits a strong vibration around 607 cm^{-1} which corresponds to antisymmetric Ti-O-Ti mode of titanium oxide [28]. The shifting of characteristics peak show a strong interaction between TiO_2 and PANI. Further, the increased shift with increasing concentration of TiO_2 indicate the possibility of formation of nanocomposite with modified absorption properties.

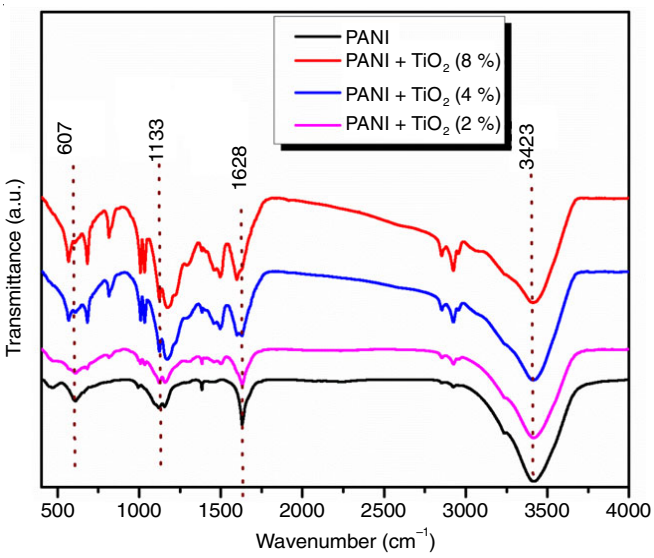

Fig. 3. FTIR spectra for PANI and PANI/TiO_2 nanocomposites

Raman spectra of pure PANI and PANI/TiO_2 nanocomposites were measured to see their vibration modes as shown in Fig. 4(a, b). It is clearly noted from Fig. 4a, PANI exhibited different vibration modes near 406, 509, 575, 825, 1183, 1249, 1341, 1507 and 1603 cm^{-1}. The peak observed at 1603 and 509 cm^{-1} for pure PANI corresponds to C=C stretching vibrations of benzenoid and quinoid rings, respectively. Whereas, C-H bending vibration of benzene quinoid ring are observed at 1341 and 1183 cm^{-1}, respectively. Incorporation of TiO_2 in PANI leads to shifting these peaks towards higher wavenumber which shows more stretching in different types of bonds. It is further evidenced that scattering of visible laser light is majorly from TiO_2 nanoparticles with a very little contribution from amorphous PANI matrix.

Thermal stability and dielectric properties: The nanocomposite is synthesized with an aim to improve the thermal stability of polyaniline. Due to the excellent thermal stability of TiO_2, the nanocomposites may found favourable to the application in the domain of sensor and optoelectronic devices [29]. The weight loss measured with temperature is indicated in Fig. 5 for pure PANI and PANI/TiO_2 (8 % w/w) up to 900 ºC. The weight loss in PANI/TiO_2 (8% w/w) within the temperature range 150-200 ºC is due to the deintercalation of water chemisorbed inTiO_2 nanoparticles. The thermal stability is evident from the relative weight loss of pure PANI and PANI/TiO_2 (8 % w/w) among which the later show lesser weight loss at higher temperatures.

Dependence of dielectric constant and loss tangent as a function of frequency is plotted for the synthesized PANI and PANI/TiO_2 nanocomposites [Fig. 6(a,b)], respectively at room temperature. It was observed that dielectric constant and dielectric loss are high at low frequency and decreases sharply as frequency increases before becoming constants at high frequencies indicating the usual dispersal. This behavior can be expl-

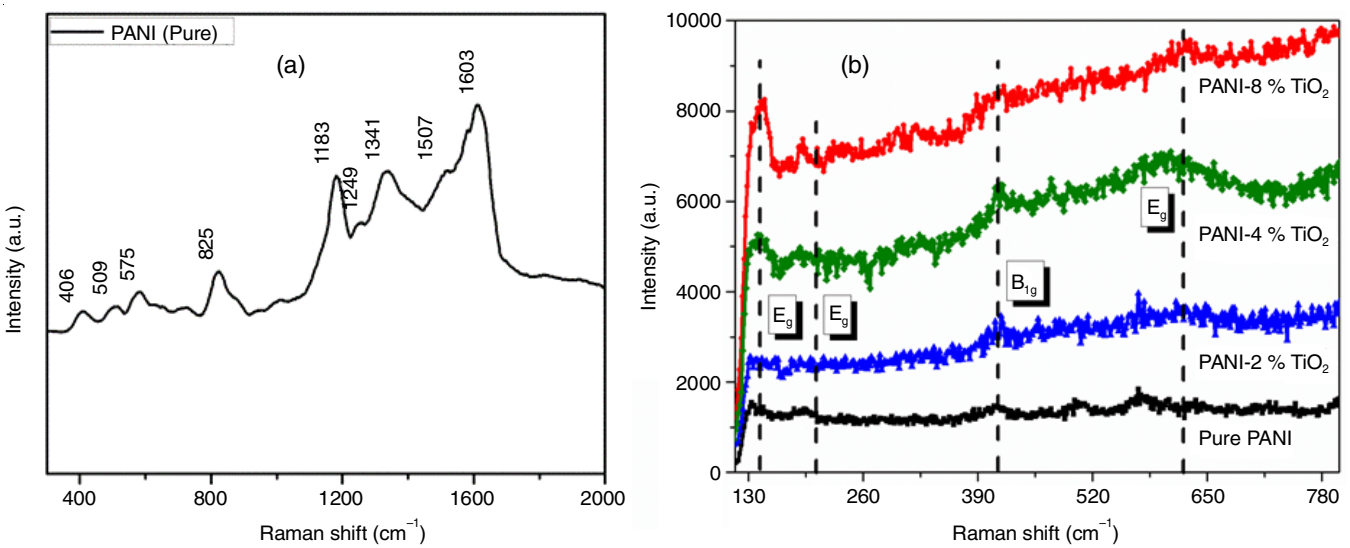

Fig. 4. (a) Raman spectra of PANI and (b) PANI/TiO_2 nanocomposites

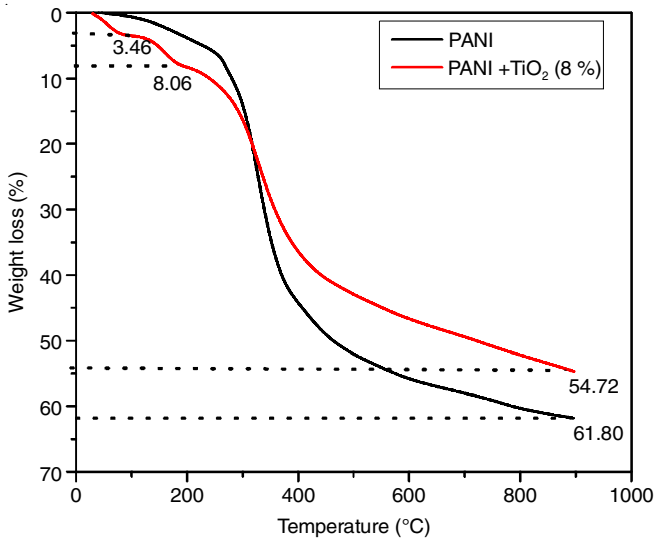

Fig. 5. TGA thermogram of PANI and PANI/TiO_2 nanocomposite

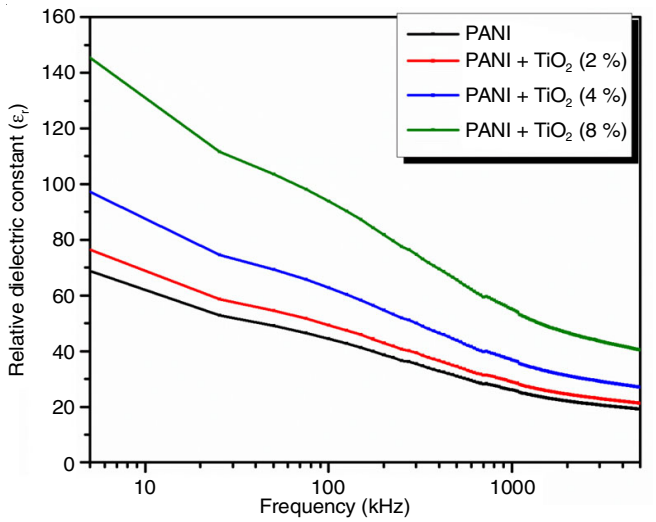

Fig. 6(a). Variation of relative dielectric constant with frequency of applied field for PANI and PANI/TiO_2 nanocomposites

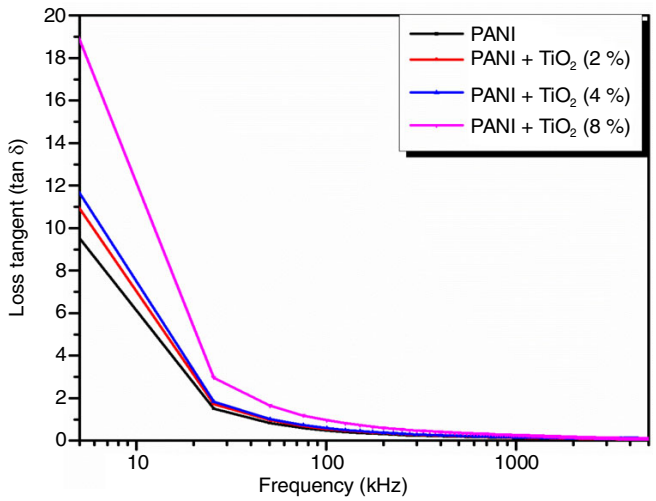

Fig. 6(b). Variation of loss tangent with frequency of applied field for PANI and PANI/TiO_2 nanocomposites

ained using Debye-like relaxation mechanism. At low frequency region dipole moment follow the applied field which causes higher value of dielectric constant but as we increase the frequency the field cannot induce the dipole moment which reduces value of dielectric constant [30-33]. As capacitance and dielectric constant are directly proportional to each other as shown by the following equation [32]:

$$\varepsilon' = \frac{C \cdot d}{A \cdot \varepsilon_o} \quad (2)$$

where C = capacitance, d = spacing between the electrodes, A = cross section area of the electrodes, ε_o = permittivity of free space and ε' = dielectric constant.

The energy lost in a dielectric is measured by the angle δ between the current and charging potential. In dielectric systems relaxation effects occur if dielectric displacement D(ω) lags behind in phase with electric field E(ω). For vacuum, this angle is 90º but if dielectric material of some dielectric constant is placed, this phase angle does not remain 90º. The angle by which dielectric displacement D(ω) deviates from 90º is termed as loss angle or tangent loss. It is the ratio of dielectric loss to the dielectric constant. The higher values of tan δ at low frequency and decrease in tan δ at higher frequency for pure PANI and PANI/TiO_2 composites of different concentration are shown in Fig. 6(b). As frequency increases, dielectric constant and loss tangent decreases sharply and hence tan δ decreases sharply. Decrease in dielectric constant and tan δ with increasing frequency is a typical characteristic of conducting polymer. Our observed measurements are in good agreement with literature [33]. Further, PANI/TiO_2 nanocomposites indicate higher dielectric constant as compared to pure PANI exhibitng a uniform increase with increase in concetration of TiO_2 in PANI/TiO_2 nanocomposites. However, higher dielectric constants are coupled with higher dielectric losses in this study.

Conclusion

PANI/TiO_2 nanocomposite samples with various concentrations of TiO_2 nanoparticles were synthesized using chemical oxidation at 0-5 ºC. The relative positions of peaks obtained from FTIR and XRD are attributed to the substantive interaction between PANI and TiO_2 nanoparticles. The SEM images helped to draw the conclusion that the increased concentration of TiO_2 had a strong effect on PANI morphology. The addition of TiO_2 in PANI shows higher thermal stability and higher dielectric constant as compare to pure PANI. The investigation of PANI/TiO_2 nanocomposites confirmed their stability and suitability for optoelectronics devices.

CONFLICT OF INTEREST

The authors declare that there is no conflict of interests regarding the publication of this article.

REFERENCES

1. A.A. Athawale and M.V. Kulkarni, *Sens. Actuators B: Chem.*, **67**, 173 (2000); https://doi.org/10.1016/S0925-4005(00)00394-4.
2. R. Nohria, R.K. Khillan, Y. Su, R. Dikshit, Y. Lvov and K. Varahramyan, *Sens. Actuators B: Chem.*, **114**, 218 (2006); https://doi.org/10.1016/j.snb.2005.04.034.
3. G.B. Shumaila, V.S. Lakshmi, M. Alam, A.M. Siddiqui, M. Zulfequar and M. Husain, *Curr. Appl. Phys.*, **11**, 217 (2010); https://doi.org/10.1016/j.cap.2010.07.010.

4. S.M. Reda and S.M. Al-Ghannam, *Adv. Mater. Phys. Chem*., **2**, 75 (2012); https://doi.org/10.4236/ampc.2012.22013.
5. K. Gupta, P.C. Jana and A.K. Meikap, *Synth. Metals*, **160**, 1566 (2010); https://doi.org/10.1016/j.synthmet.2010.05.026.
6. W.J. Bae, K.H. Kim and W.H. Jo, *Macromolecules*, **37**, 9850 (2004); https://doi.org/10.1021/ma048829b.
7. W.M.A.T. Bandara, D.M.M. Krishantha, J.S.H.Q. Perera, R.M.G. Rajapakse and D.T.B. Tennakoon, *J. Compos. Mater*., **39**, 759 (2005); https://doi.org/10.1177/0021998305048155.
8. P. Aranda, M. Darder, R. Fernandez-Saavedra, M. Lopez-Blanco and E. Ruiz-Hitzky, *Thin Solid Films,* **495**, 104 (2006); https://doi.org/10.1016/j.tsf.2005.08.284.
9. J.H. Sung and H.J. Choi, *J. Macromol. Sci. B: Phys*., **44**, 365 (2005); https://doi.org/10.1081/MB-200057348.
10. A. Dey, S. De, A. De and S.K. De, *Nanotechnology*, **15**, 1277 (2004); https://doi.org/10.1088/0957-4484/15/9/028.
11. C. Huang and Q.M. Zhang, *Adv. Mater.*, **17**, 1153 (2005); https://doi.org/10.1002/adma.200401161.
12. J. Gao, J.M. Sansiena and H. L. Wang, *Synth. Metals*, **135**, 809 (2003); https://doi.org/10.1016/S0379-6779(02)00883-4.
13. E.W. Paul, A.J. Riccio and M.S. Wrighton, *J. Phys. Chem.*, **89**, 1441 (1985); https://doi.org/10.1021/j100254a028.
14. Z.-L. Hua, J.-L. Shi , L.-X. Zhang, M.-L. Ruan and J.-N. Yan, *Adv. Mater.*, **14**, 830 (2002); https://doi.org/10.1002/1521-4095(20020605)14:11<830::AID-ADMA830>3.0.CO;2-W.
15. A. Rothschold and Y. Komem, *Appl. Phys. Lett*., **82**, 574 (2003); https://doi.org/10.1063/1.1539556.
16. S. Stankovich, D.A. Dikin, G.H.B. Dommett, K.M. Kohlhaas, E.J. Zimney, E.A. Stach, R.D. Piner, S.T. Nguyen and R.S. Ruoff, *Nature*, **442**, 282 (2006); https://doi.org/10.1038/nature04969.
17. J. Wu, W. Pisula and K. Müllen, *Chem. Rev*., **107**, 718 (2007); https://doi.org/10.1021/cr068010r.
18. X. Wang, L. Zhi and K. Mullen, *Nano Lett*., **8**, 323 (2008); https://doi.org/10.1021/nl072838r.
19. Asha, S.L. Goyal, S. Kumar and N. Kishor, *Indian J. Pure Appl. Phys.*, **52**, 341 (2014); http://nopr.niscair.res.in/handle/123456789/28703.
20. A.F. Khan, M. Mehmood, S.K. Durrani, M.L. Ali and N.A. Rahim, *Mater. Sci. Semicond. Process*., **29**, 161 (2015); https://doi.org/10.1016/j.mssp.2014.02.009.
21. R. Ganesan and A. Gedanken, *Nanotechnology*, **19**, 435709 (2008); https://doi.org/10.1088/0957-4484/19/43/435709.
22. M. Diantoro, M. Z. Masrul and A. Taufiq, *IOP Conf. Series: J. Physics Conf. Series*, **1011**, 012065 (2018); https://doi.org/10.1088/1742-6596/1011/1/012065.
23. S. Srivastava, S.S. Sharma, S. Kumar, S. Agrawal, M. Singh and Y.K. Vijay, *Int. J. Hydrogen Energy*, **34**, 8444 (2009); https://doi.org/10.1016/j.ijhydene.2009.08.017.
24. S. Srivastava, S.S. Sharma, S. Kumar, S. Agrawal, M. Singh and Y.K. Vijay, *Synth. Metals*, **160**, 529 (2010); https://doi.org/10.1016/j.synthmet.2009.11.022.
25. B. Butoi, A. Groza, P. Dinca, A. Balan and V. Barna, *Polymers*, **9**, 732 (2017); https://doi.org/10.3390/polym9120732.
26. T.C. Mo, H.W. Wang, S.Y. Chen and Y.C. Yeh, *Ceramics Int*., **34**, 1767 (2008); https://doi.org/10.1016/j.ceramint.2007.06.002.
27. S. Deivanayaki, V. Ponnuswamy, S. Ashokan, P. Jayamurugan and R. Mariappan, *Mater. Sci. Semicond. Process.*, **16**, 554 (2013); https://doi.org/10.1016/j.mssp.2012.07.004.
28. J. Yu, C.Y. Jimmy, W. Ho and Z. Jiang, *New J. Chem*., **26**, 607 (2002); https://doi.org/10.1039/B200964A.
29. D.C. Schnitzler, M.S. Meruvia, I.A. Hummelgen and A.J.G. Zarbin, *Chem. Mater.*, **15**, 4658 (2003); https://doi.org/10.1021/cm034292p.
30. J. Lu, K.S. Moon, B.K. Kim and C.P. Wong, *Polymer*, **48**, 1510 (2007); https://doi.org/10.1016/j.polymer.2007.01.057.
31. B.G. Soares, M.E. Leyva, G.M.O. Barra and D. Khastgir, *Eur. Polym. J.*, **42**, 676 (2006); https://doi.org/10.1016/j.eurpolymj.2005.08.013.
32. X.Z. Yan and T. Goodson, *J. Phys. Chem. B*, **110**, 14667 (2006); https://doi.org/10.1021/jp061522p.
33. M. Irfan, A. Shakoor, B. Ali, A. Elahi, Tahira, M.I. Ghouri and A. Ali, *Eur. Acad. Res.*, **2**, 10602 (2014).